https://doi.org/10.31436/iiumej.v25i2.3094

PERFORMANCE ANALYSIS OF AN INDUCTION MOTOR COUPLED VIF WITH MR FLUID DAMPER

SYED MUNIMUS SALAM, MUHAMMAD MAHBUBUR RASHID*

Department of Mechatronics Engineering, International Islamic University Malaysia, Kuala Lumpur, Malaysia

**Corresponding author: mahbub@iium.edu.my*

(Received: 3 November 2023; Accepted: 6 March 2024; Published online: 15 July 2024)

ABSTRACT: The flywheel is a classic mechanical device that is often used to enhance the rotational motion of engines. Electrical machines often face fluctuations in speed that hamper speed stability and cause extra power consumption. Recently, a few publications have analyzed the impact of the flywheel to reduce fluctuation and energy consumption in electric motors. This study proposes the use of a flywheel with a changeable moment of inertia, which can be manipulated to boost both speed stability and energy efficiency. The objective is to improve the speed stability of industrial motors in the presence of the loading effect. This study introduces a magneto-rheological variable inertia flywheel (MRVIF) to control rotational speed and reduce power usage. The purpose of analytical development is to assess the influence of rotational speed and excitation current on the MR damper's moment of inertia for control purposes. The investigation focuses on the analysis of power usage and stability across different power inputs and rotating speeds. The effectiveness of the suggested MRVIF was evaluated via the development of a prototype. Experiments were undertaken to validate the effectiveness and stability of the system. The findings illustrate the potential use of MRVIF in reducing energy consumption and enhancing speed stability.

ABSTRAK: 'Flywheel' atau roda tenaga adalah peranti mekanikal klasik yang sering digunakan bagi meningkatkan gerakan putaran enjin. Mesin elektrik sering menghadapi turun naik kelajuan yang menghalang kestabilan kelajuan dan menyebabkan penggunaan kuasa tambahan. Baru-baru ini, terdapat beberapa kajian terdahulu yang menganalisis kesan roda tenaga bagi mengurangkan turun naik dan penggunaan tenaga dalam motor elektrik. Kajian ini mencadangkan penggunaan roda tenaga dengan momen inersia boleh ubah, di mana ia boleh dimanipulasi bagi meningkatkan kestabilan kelajuan dan kecekapan tenaga. Objektif kajian adalah bagi meningkatkan kestabilan kelajuan motor industri bersama kesan muatan. Kajian ini memperkenalkan pembolehubah magnetorheologikal roda tenaga inersia (MRVIF) bagi mengawal kelajuan putaran dan mengurangkan penggunaan kuasa. Tujuan pembangunan analitikal ini adalah bagi menilai pengaruh kelajuan putaran dan arus pengujaan pada momen inersia peredam MR bagi tujuan kawalan. Kajian memfokuskan pada analisis penggunaan kuasa dan kestabilan merentas pelbagai input kuasa dan kelajuan putaran. Keberkesanan MRVIF yang dicadangkan telah diuji melalui pembangunan prototaip. Eksperimen dijalankan bagi mengesahkan keberkesanan dan kestabilan sistem. Penemuan ini menggambarkan potensi MRVIF dalam mengurangkan penggunaan tenaga dan meningkatkan kestabilan kelajuan.

KEYWORDS: *Variable Inertia Flywheel; Energy Saving; Magneto Rheological Fluid.*

https://doi.org/10.31436/iiumej.v25i2.3094

1. INTRODUCTION

A flywheel with variable inertia requires a more complex design compared to one with constant inertia. For a flywheel to possess a controlled moment of inertia along its rotating axis, it is necessary for the flywheel to have a flexible geometry around it. Furthermore, any changes made to the geometry of the flywheel need the movement of parts inside it. Because of its higher level of complexity, a variable inertia flywheel (VIF) may make more efficient use of energy saved per unit than a conventional fixed inertia flywheel. Nevertheless, when the flywheel of a machine is substituted with the VIF, the additional mass of the VIF might still lead to a configuration that has a higher energy density in comparison to its fixed inertia equivalent [1].

The coefficient of variance is a measure used to characterize the variation in angular velocity of a flywheel across a cycle relative to its average angular velocity. A system using a conventional flywheel is used to minimize fluctuations in angular velocity. A high moment of inertia is necessary to get a low coefficient of fluctuation. An adjustable inertia flywheel might be quite advantageous in this situation [2].

The energy-saving capacity of the flywheel has gained significant interest in recent years. Jauch developed a flywheel energy storage system that was integrated into the rotor of a wind turbine [3]. Another study developed a flywheel that was directly coupled to an engine and had a changeable inertia due to the use of springs. The flywheel offers a wide range of energy storage choices while simultaneously preserving its rotational speed [4]. The double-mass flywheel incorporated a centrifugal pendulum devised by Ishida et al. [5]. The variable inertia developed by the fluid of a flywheel proposed by James et al. had the capability to maintain a consistent rotational speed across a wide range for energy storing [6]. According to Yuan L et al., the variable inertia flywheel may take the role of the conventional fixed inertia flywheel [7]. In a similar study, a flywheel was considered without any fixed adjustment to the system's input shaft, along with a variable moment of inertia of the mass. By utilizing a fluid that behaved like a series of inertia masses, Matsuoka presented new vibration reduction systems. On the other hand, the usage of magnetorheological fluid in flywheels has not been very common [8]. The energy-saving potential of VIMRF (variable inertia magnetic rheological flywheel), in contrast to competitors, has not yet been fully explored. Alternative methods are developing with respect to research progress. Without taking into account the impact of high system stability, the majority of the research in [9] concentrated on the design and implementation of VIF in the field of power savings and stability.

Improving overall operating efficiency and sustainability in industrial motors requires addressing the problems of speed stability and energy usage. Increased speed stability lowers the possibility of interruptions and defective products in industrial operations by ensuring steady and dependable performance. Simultaneously, reducing energy use reduces operating expenses and supports international environmental responsibility programs. Improved motor efficiency supports regulatory compliance and places companies positively in the context of changing environmental requirements by helping to minimize carbon emissions and energy waste. Overall, putting energy efficiency and speed stability first in industrial motors not only makes them more economically viable but also shows that the company is committed to using sustainable and ethical manufacturing techniques.

The inertia control of a VIF may be unpredictable under conditions of load disruptions, which can cause instability and system failure. The possible weakness of the strategies is the lack of concentration on inertia control. All previous variable inertia control designs and methodologies do not even provide stable control without considering the consequences of the

applied device. Lack of control on a variable inertia flywheel's moment of inertia causes additional energy loss. Modeling a system with proper control of variable inertia is challenging. Moreover, implementing a strong adaptive control approach for any unexpected changes in the applied machine with significant stability and energy savings is more crucial.

The main objective of this study is to analyze the performance of a developed MR VIF coupled induction motor prototype to find out the impact of the MR fluid properties on energy consumption and speed stability of the induction motor.

2. THE METHOD OF VARIABLE INERTIA CONTROL OF A FLYWHEEL

A flywheel with variable inertia inherently requires a significantly intricate construction compared to a flywheel with static inertia. The change in velocity of an object's mass produces a force of inertia that counteracts the object's flexibility, leading to the generation of preserving forces. Consequently, when external disturbances affect a body, its inertia and inner preserving forces result in unwanted oscillation. The kind of vibration (linear, torsional, or bending) depends on the design of the machine. Vibration poses a substantial issue in all mechanical systems, as it may have adverse effects on the machine's durability, product excellence, and overall safety. In addition, it has the potential to cause structural disruption [10]. Hence, the act of reducing and regulating vibrating is an essential effort. The essential elements of vibratory systems consist of the spring, damper, and mass. The efficient design, optimization, and exact production of these three components are crucial to the development of an efficient vibration isolation system [11].

Vibration is a frequent motion phenomenon that often oscillates around a balancing position in both the flywheel and inertia mass. In some normal scenarios, vibration can be required when it comes to anything from little devices like loudspeakers to huge ones like tamping machines, vibrating conveyors, and sieves. High levels of vibration may sometimes be advantageous and desired. However, vibration in VIF is generally undesirable because it makes annoying noise, consumes energy, leads to mechanical wear and structural stress, and increases risk. As a result, experts have devoted a lot of time to studying vibration control. Here, the term "vibration control" refers to the reduction of vibration to lessen unwelcome oscillations in a protected structure. Typically, a compact connecting element made up of a spring, damper, or mass accomplishes this [12].

Various ideas for reducing vibration exist for managing vibrations of the specified sort, depending on the need for external power or information. The exploration of three vibration-controlling mechanisms, namely passive, semi-active, and active systems, has taken place in recent decades. These systems are often known as vibration control systems [13]. Vibration is typically undesirable when it causes annoying commotion, results in peril, or dissipates energy. As a result, researchers have always been interested in vibration control. Research in recent decades has mostly focused on active, passive, and semi-active vibration control systems. The stiffness of these components greatly influences their reaction, including responding time and operational frequency range. Semi-active control is characterized by a reduced reliance on outside force as control energy, resulting in increased stability compared to active control. Additionally, it has a broader range and greater adaptability compared to passive control. Hence, semi-active control systems are very intriguing and find application in several technical fields. For semi-active control, variables can be mass, rigidity, or damping [14].

The earliest vibration control technique is passive control, which receives no energy or information from the outside world. A passive system has the benefits of simple construction,

cheap cost, stability, and high dependability. Still, it also falls short since it can't adapt its structural parameters to changes in vibration over time and can't adapt its design to different excitation frequencies. Active control uses an actuator, driven by external energy and control information, to create an additional vibration channel. This enables the exact and quick modification of the external force of an outside interruption for the purpose of reducing vibration. This gadget, under an active control system, has the capacity to augment or diminish mechanical energy immediately. Specifically, the main vibration is paired with an input that has the same amplitude but the opposite phase, canceling both vibrations [15].

Semi-active devices are unable to input energy into a system that they are controlling directly. This crucial requirement makes sure that changes in the system parameters do not result in parametric excitation. When employing the word "semi-active" in literature, this is often not taken into appropriate consideration. It has been shown to function better than a system with passive control and is utilized as an effective method to reduce unwelcome oscillations in many applications. Active vibration control is, however, overshadowed by the system's relative expense, complexity, and instability [16].

A Semi-active damper can be called a hydro-mechanical controlling system that could modulate energy dissipation with little electrical power consumption. For instance, hydraulic dampers are constructed to exert a force that is directly proportionate to the velocity. These devices enhance the range of damping characteristics that may be achieved with a regular (passive) damper. Various energy-dissipating gadgets have been used to provide the necessary damping force for semi-active damping control.

A magnetorheological (MR) or electrorheological (ER) damper is composed of a hydraulic cylinder that contains polarizable particles in an MR or ER fluid, often oil, with particle sizes in the micron range. Non-Newtonian fluids, such as MR and ER fluids, undergo changes in their properties when subjected to electric or magnetic fields. Micron-sized iron particles, when suspended in a carrier fluid such as water, petroleum-based oil, or silicon-based oil, may change the flow properties of the fluid by arranging themselves in chain-like patterns along the lines of magnetic or electrical fields. Both MR and ER materials may rapidly transition from a fluid state to a semi-solid state within milliseconds when exposed to a magnetic or electric field. Since they don't have any moving components, MR and ER dampers are mechanically dependable [17].

The moment of inertia grows when the flywheel spins rapidly because the variable masses have shifted to the flywheel's radius. However, if the flywheel's varying masses are allowed to oscillate freely, the system will cause vibration and instability. Spring forces are applied as a dampening force to prevent this from happening. There is not enough resistance here to maintain a steady state. Low-speed operation further complicates mass position control. By introducing MR fluid into the cavity, the viscosity may be modulated by external stimulation, allowing for precise manipulation of the mass's location.

3. VIF MODELLING WITH MR FLUID

When the slider is moved along the slot, the flywheel's inertia changes accordingly. Figure 1 is a diagrammatic representation of the variable inertial flywheel. When the flywheel is spinning at 0 RPM, the springs are at full extension and contacting the hub. In this case, we ignore the pull of gravity. The springs are fixed in their length and can only be compressed. The VIF is composed of a compact circular disc, including four sliders and four springs. The spinning of the flywheel induces the displacement of slides along the slots. The compression

https://doi.org/10.31436/iiumej.v25i2.3094

of the springs up to their maximum length is determined by the speed of the flywheel. The movement of the sliders inside the slots causes the moment of inertia of the flywheel to vary.

Considering the slider's moment of inertia, it can be expressed for the slider's own mass center, while the flywheel fixed structural part's moment of inertia around the shaft center is

$$J_{slide} = \frac{1}{4} m_{slide} \left(\frac{D_{slide}^2}{4} + \frac{L_{slide}^2}{3} \right) \quad (1)$$

$$J_{flywheel} = J_{solid} + n_{slide} * J_{slide} \quad (2)$$

where m_{slide}, D_{slide} and L_{slide} are the mass, diameter, and length of the slider. n_{slide} represents the number of slots available in the flywheel.

The following expression describes the calculation procedure for the moments of inertia of the solid part of the flywheel, considering a fan-shaped body.

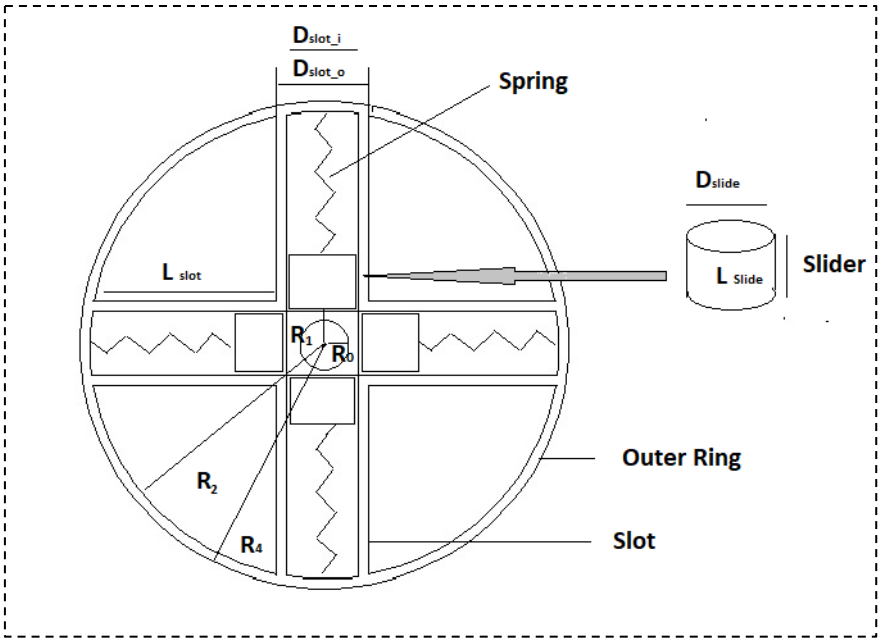

Figure 1. Schematic diagram of VIF system.

$$J_{full} = \int_{R_0}^{R_4} r^2 dm = \int_{R_0}^{R_4} 2\pi H r^3 \rho dr = \frac{1}{2} \pi H \rho (R_4^2 - R_0^2) \quad (3)$$

$$J_{hole} = \int_{R_1}^{R_2} r^2 dm = \int_{R_1}^{R_2} 2\pi H \left(r - \frac{\sqrt{2}}{2} D_{slot_O} \right) r^2 \rho dr$$

$$= \pi H \rho \left(\frac{1}{8} (R_2^2 - R_1^2) - \frac{\sqrt{2}}{12} D_{slot_O} (R_2^2 - R_1^2) \right) \quad (4)$$

Again, here moment of inertia of the slot is calculated as

$$J_{slot} = \frac{1}{12} \rho (L_{slot}^2 + D_{slotI}^2)^2 \quad (5)$$

Finally, the value of J_solid can be obtained by,

$$J_{solid} = J_{full} - n_{slide} * (J_{hole} + J_{slot}) \quad (6)$$

As the flywheel spins, the slider slides along the slot.

4. Simulation Modelling of The System

In the second step, a simulation system has been developed for testing the proposed theory. To analyze the complex changing aspects of the induction motor with the MR VIF and the VIF, the system model is constructed utilizing the systematic bond graph approach [18].

This method is a self-contained construction of a conventional method that relies especially on a constant type of energy interchange in an integrated manner. The sliders' maximum displacement is limited by the fixed outside boundary ring of the constructed flywheel, which is closely attached to the main frame of this flywheel. The sliders are housed inside the cylindrical slots. The sliders are encircled by a coil at the outer periphery. The condition of the MR fluid inside the slot undergoes a change when it is stimulated by external power. During the normal VIF operation, the cylindrical springs are extracted while the sliders inside the cylinder are securely immobilized with the frame of the flywheel. The flywheel rpm is detected using a special non-contact rpm sensor and is communicated to the data logger.

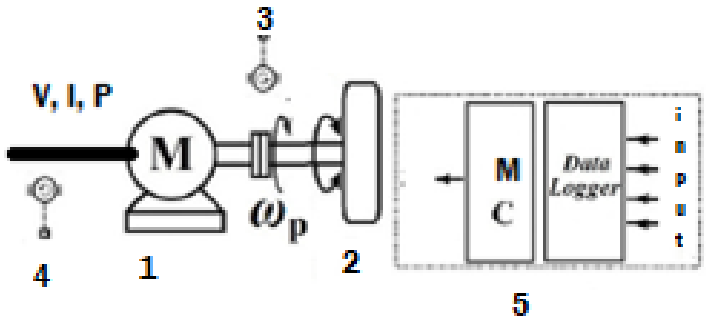

System Componenets

1. Induction Motor
2. Flywheel
3. Speed Sendor
4. Voltage, Current, Power, Temperature Sensor
5. MR Exciter

Figure 2. Schematic diagram of IM coupled VIF system.

In the Figure 2, the schematic diagram of the system utilized for the IM coupled VIF is illustrated. The basic system model consists of the induction motor (1) and the flywheel (2). The system parameters that are considered as inputs are voltage current and power, and the output parameters that are observed for control are the speed and temperature. The Magneto rheological cylinder excitation can change the viscosity of the MR fluid, which can control the VIF semi-actively. In addition to the structural characteristics of the flywheels, the model considers the qualities of MR fluid, variations in viscosity, and the induction motor. The following assumptions are made:

- The fluid inertia is ignored.
- The fluid is classified as Newtonian.
- The spring's properties are assumed to be linear, and the model does not consider the dynamics of the springs.
- The gravitational force acting on the slider is not considered.

https://doi.org/10.31436/iiumej.v25i2.3094

The effect of excitation current and rotational speed on the moment of inertia of a Magnetorheological (MR) damper is typically investigated using both computational and experimental techniques. Dynamic testing sensors, which measure the moments of inertia produced by exposing the damper to a range of rotational speeds and excitation currents, are a common component of experimental approaches. Computational techniques replicate the behavior of the MR damper under various operating situations using simulation modeling and finite element analysis. Through the optimization and design of MR damper systems, these analytical techniques assist in understanding how variations in rotational speed and excitation current affect the moment of inertia.

Notably, for modeling electromagnetic machines and their rotating magnetic fields, the support for vector variables is crucial. Existing bond graph simulation tools only accommodate scalar variables, prompting our proposal for an innovative approach. We suggest introducing support for complex variables and vectors in bond graphs to facilitate the modeling of polyphase electromagnetic and spatial vector systems. To address this, we have introduced a rotary gyrator element and incorporated it with a switched junction to formulate a toolbox supporting complex and vector variables. This approach is implemented by creating a complex S-function toolbox in Simscape within the MATLAB environment, chosen to leverage the speed of S-functions, the user-friendly nature of Simulink, and the widespread popularity of MATLAB. The spring remains undeformed at its minimal length ($lmin$).

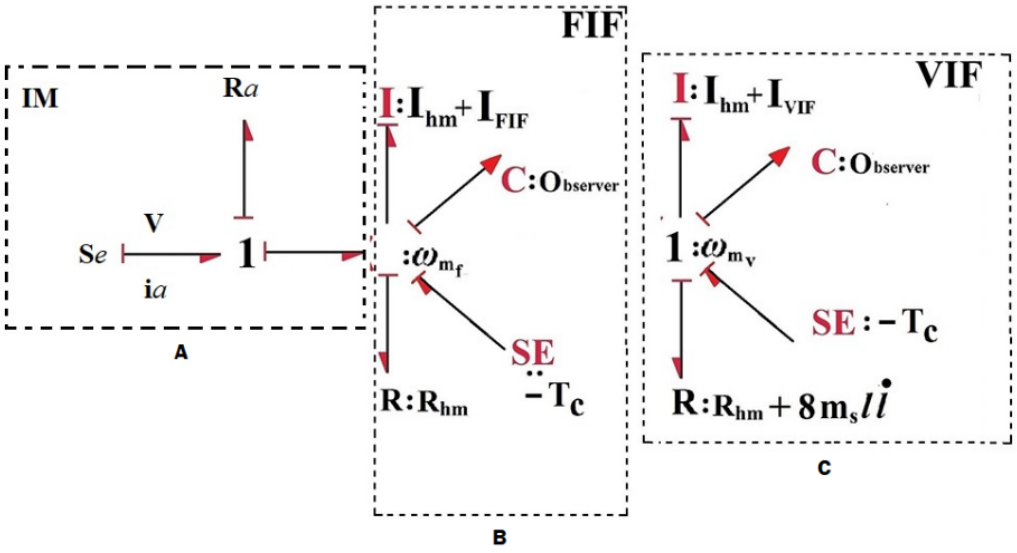

Figure 3. Bond graph representation

Figure 3 depicts the bond graph concept model of the induction motor drive system, including the flywheel. The sub-models of the induction motor, flywheel inertia factor (FIF), and voltage inverter factor (VIF) are labeled as A, B, and C, respectively, to enhance clarity.

The source of flow (SF) element is the electrical power that develops the rotary velocity of the motor (ωmf). A motor-coupled shaft converts electrical energy into mechanical energy or vice versa. Ultimately, a Simulink simulation has been created to assess the MR VIF system using the bond graph correlation and equation. Figure 4 depicts the system, and simulations have been conducted under various scenarios. The data has been compared to the authentic data generated using a similar configuration, and subsequently, an error analysis has been conducted to enhance the results further.

https://doi.org/10.31436/iiumej.v25i2.3094

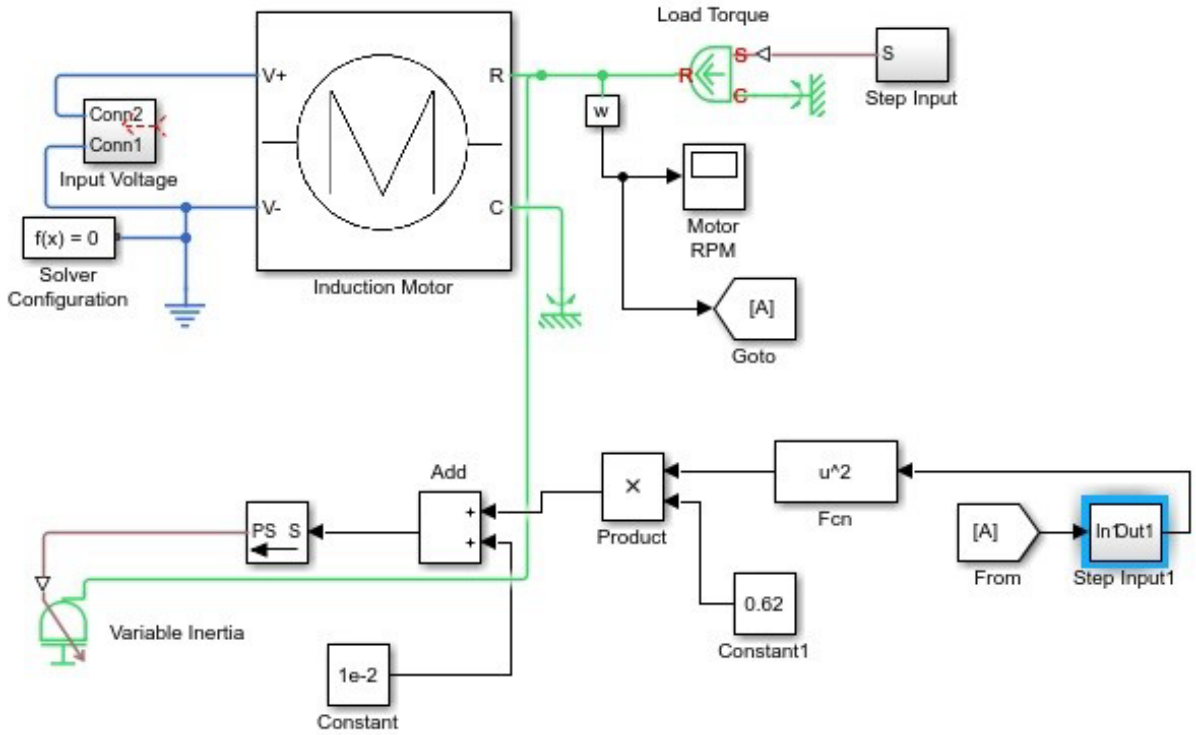

Figure 4. Simulink simulation representation

5. PROTOTYPING A MR VIF SYSTEM COUPLED WITH IM

A prototype made of aluminum was created in the beginning for testing purposes. The primary motivation for using aluminum was to prevent magnetic field induction. The fly-wheel cage was designed by the criteria given in Table 1. In certain circumstances, the value of some parameters was modified for analysis purposes. An induction motor applies the flywheel system.

Table 1. Construction details of MRVIF

Parts and Accessories	Properties
Frame	Aluminium Alloy
Slider	Iron casting
Cylinder	Stainless Steel
Spring	Steel
MR Fluid	Black Iron Dust with Silica Oil
Coil	Copper
Cable	DC cable
Brush	Carbon Brush
Base	Steel sheet

The characteristics of the electrical system have been tested using an electric multi-meter, and the system's speed is controlled by a converter. The converter primarily adjusts current and power to bring about the desired change in velocity. Figure 5 displays the physical system that is being examined in this research. A variable-speed electric motor controller is used to operate an induction motor in the system.

The induction motor has been connected to the flywheel constructed from an aluminum alloy (1), which is positioned on the base (5). The changing inertia mass is contained within the cylinder housing the MR (Magnetorheological) fluid (2). To excite the MR fluid, a slip ring

https://doi.org/10.31436/iiumej.v25i2.3094

(3) is attached to the carbon brush to supply power to the coil within the cylinder, thereby modifying the properties of the MR fluid (4).

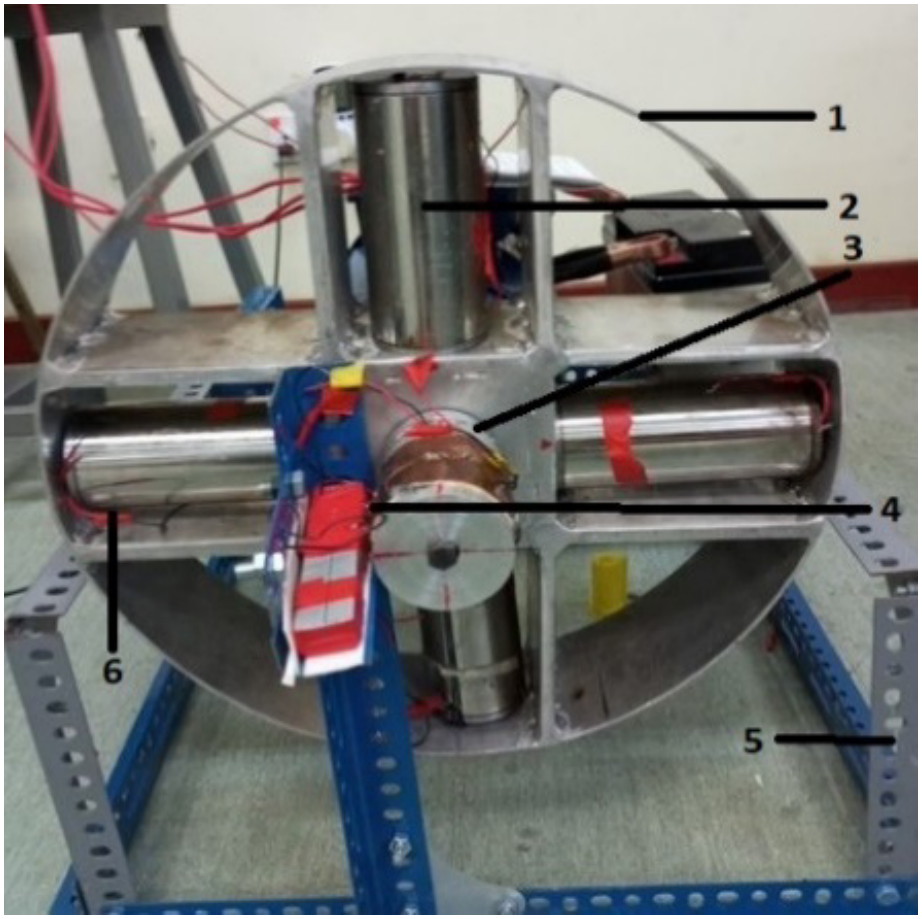

Figure 5. Prototype model representation

To ensure the maintenance of the MR fluid, each cylinder is equipped with an additional cover (6). The controller adjusts the current consumption to modulate and change the speed of the motor. It can both reverse and forward the direction of the motor's speed. The induction motor is connected to a flywheel.

The induction motor speed is regulated by supplying variable power flow via regulation of the command signal applied to the controller. The primary function of the induction motor is to power the inertia load. An analysis is conducted on the system's performance at different speeds, including both constant and changing inertia loads. Figure 6 shows the working procedure of the MR VIF with the flow chart.

To achieve the desired configuration of a cylinder with variable inertia, a hollow cylinder is equipped with a spring and a mass. The flow chart in Figure 6 shows the specific working process applied to the flywheel and controlling requirement of the system. The cylindrical structure is comprised of an internal volume containing magnetorheological (MR) fluid. The MR fluid is synthesised in a laboratory setting by combining black iron oxide (Fe_3O_4) dust with silica oil as a carrier. The resulting mixture utilises a semi-active substance, which exhibits a viscosity ranging from 0.21 to 0.27 Pas at a temperature of 30 degrees Celsius. To manipulate the MR characteristics of the fluid, an externally generated magnetic field is used as a means of exciting the fluid. Additionally, the viscosity was assessed inside the laboratory setting,

revealing a variation of 0.06 Pas when a magnetic field was applied. The table includes all the components used for manipulating inertia.

For data collection, a lab set up was installed with different data collection equipment. As discussed earlier, the electrical readings were taken by integrated multi electric meter. The speed of the system was measured using a digital tachometer. For avoiding any confusion and error, similar data was taken several times

6. PERFORMANCE ANALYSIS OF THE MODEL

To validate the model with three different viscosities of the MR fluid, the rpm of the induction motor was varied from 300 to 900 rpm. The simulated result and the experimental data were analyzed using the rpm change at the start of the induction motor. Three cases were considered for the system model:

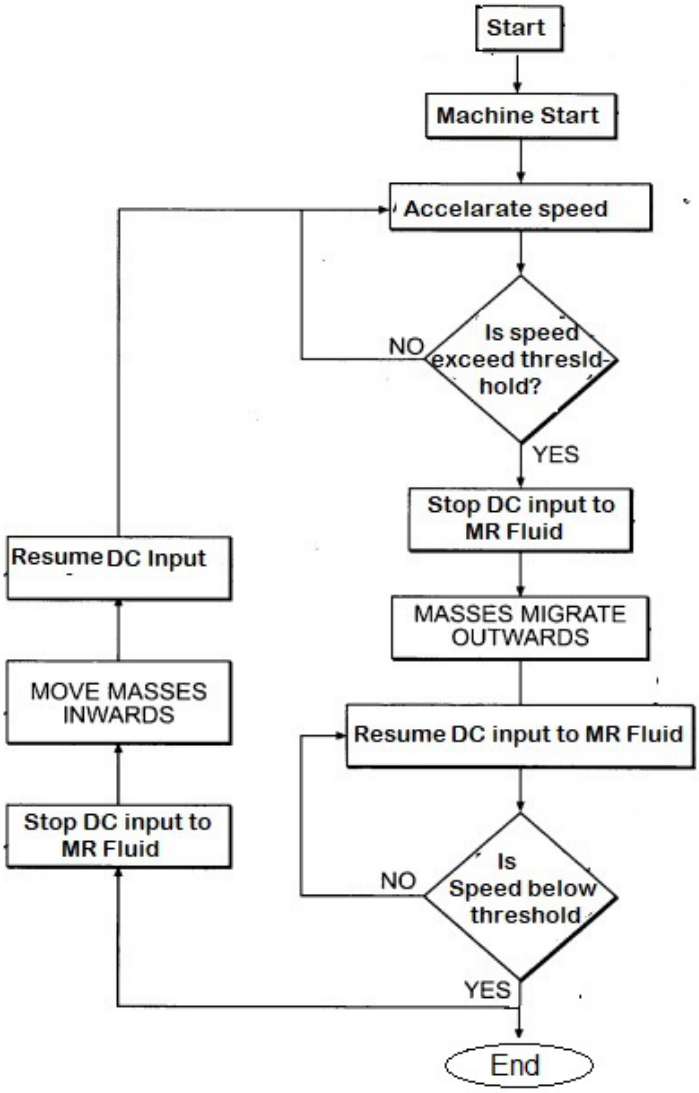

Figure 6. Flow chart used with the system model

Case 1: The motor started and the speed increased up to the highest possible changes in the supplied power to the induction motor driving the VIF with low excitation current with viscosity 0.21 to 0.23 Pas. This was achieved by giving the input power from the controller applied to the induction motor when the speed increment was done.

https://doi.org/10.31436/iiumej.v25i2.3094

Case 2: In this case, the speed of the motor driving the VIF with regular temperature and with medium viscosity is 0.24 to 0.25 Pas. It was achieved by giving the input power from the controller applied to the induction motor, then the speed increment was similarly done.

Case 3: In this case, the rpm of the induction motor is altered during running the VIF with a relatively high viscosity of 0.25 to 0.27 Pas at a regular temperature. This is achieved by applying the input power from the controller to the induction motor and then incrementing the speed similarly.

6.1. Speed Stability Analysis of the Model

A comparative analysis was conducted between the MR VIF and VIF setups. When the VIF was set up with MR fluid, the simulation results showed that the inclusion of MR fluid reduced oscillation, leading to improved speed stability and reduced overshooting. The viscosity value was augmented by the incremental damping factor for simulation purposes. The variation in the speed buildup characteristics is illustrated in Figure 7. The excitation amplitude for three separate situations was chosen to remain constant during the observation period. The induction motor was maintained at an optimal level, neither too low nor too high, as the slides could not overcome friction if the speed were low.

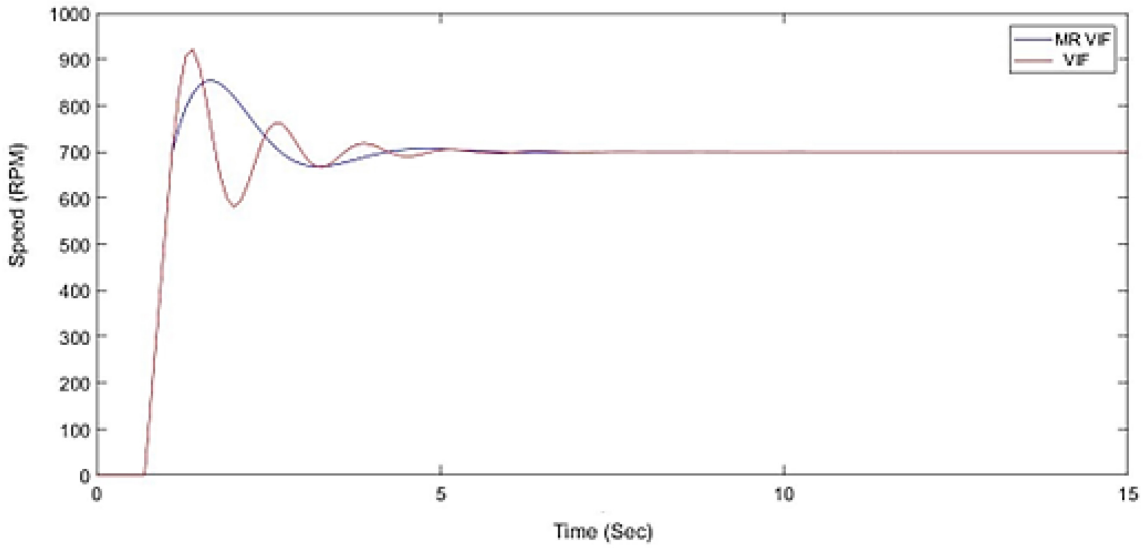

Figure 7. Speed stability analysis for MR VIF and VIF

If the speed was excessively high, there may not be sufficient viscosity to keep the sliders in the VIF and the entire flywheel would function as FIF. Hence, the maximum and minimum speed values were determined through multiple iterations of the experiment. The relative investigation of the output rpm of the induction motor driving the MRVIF and the VIF was conducted using the same process. Numerical solutions for the model equations provided in the section are obtained using software [19].

The validation of the system model was achieved through a direct comparison between the measured responses and the expected outcomes. During the testing, the input power remained constant at the early stage. Figure 7–9 illustrates the contrasting responses of the induction motor speed when driven by VIF and FIF in various scenarios. When the induction motor operated with the MR VIF, the inertia of the flywheel fluctuated in response to the motor's changing speed. Thus, when comparing the FIF to the MR VIF, the induction motor's top speed was decreased due to the growing inertial load.

https://doi.org/10.31436/iiumej.v25i2.3094

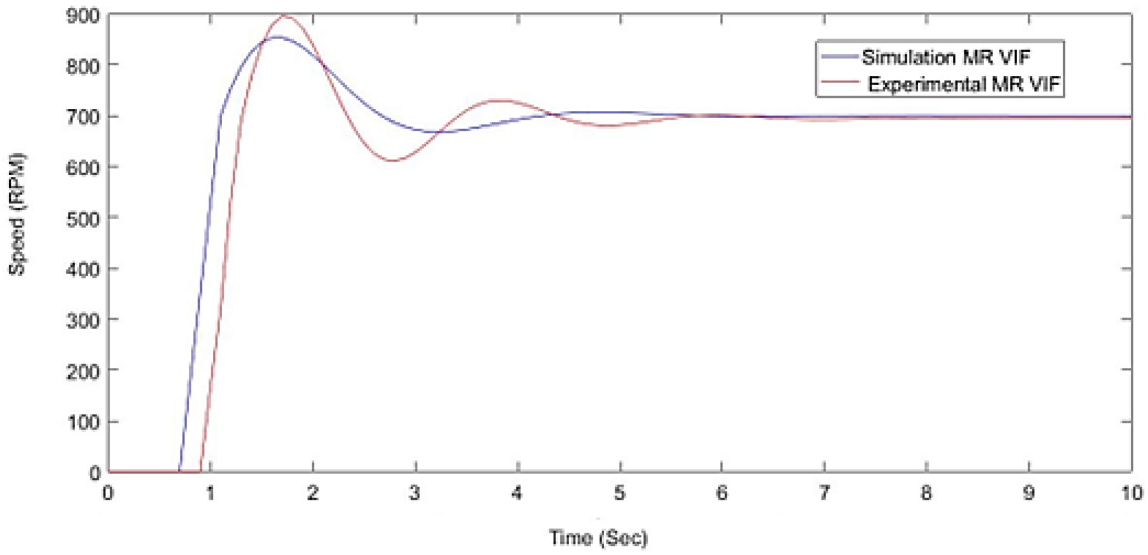

Figure 8. Speed stability analysis for simulation and experimental MRVIF

Figure 8 illustrates the comparison between the expected speed and the experimental speed of the induction motor while it was driving the MR VIF during the starting phase. The inertia of the flywheel changed in response to the varying speed of the induction motor when it was being driven using the VIF. Consequently, the peak speed of the hydraulic motor that drove the VIF was reduced due to the growing inertial load compared to the FIF. Figure 7 presents a comparison between the projected speeds using MR VIF and VIF. The Russell error approach was employed to approximate the discrepancy between the experimental and simulated responses. Equations (7) and (8) were utilized to calculate the magnitude, phase, and comprehensive errors for the speed response of the VIF and the MR VIF, respectively [20]. The magnitude error (e_m) of the experimental and simulation data was determined by,

$$\mathrm{e_m} = \mathrm{Sgn}(\mathrm{e_{rm}})\log_{10}(1 + |\mathrm{e_{rm}}|) \tag{7}$$

and

$$\mathrm{e_{rm}} = \frac{\sum_{k=1}^{n} \mathrm{M_k} - \sum_{k=1}^{n} \mathrm{D_k}}{\sum_{k=1}^{n} \mathrm{M_k}\ \mathrm{X} \sum_{k=1}^{n} \mathrm{D_k}} \tag{8}$$

where, $\mathrm{e_{rm}}$, M, and D are the relative magnitude of error and simulation data magnitude, and experimental data magnitude. The Simulink simulation and the real-time experiment were performed considering a sample time of 10ms, and a minimum sample rate was maintained at 1000. Equations (7) and (8) were used to estimate the magnitude error (e_m) as 1.411 and 0.0352 for the MR VIF and the VIF speed response, respectively.

https://doi.org/10.31436/iiumej.v25i2.3094

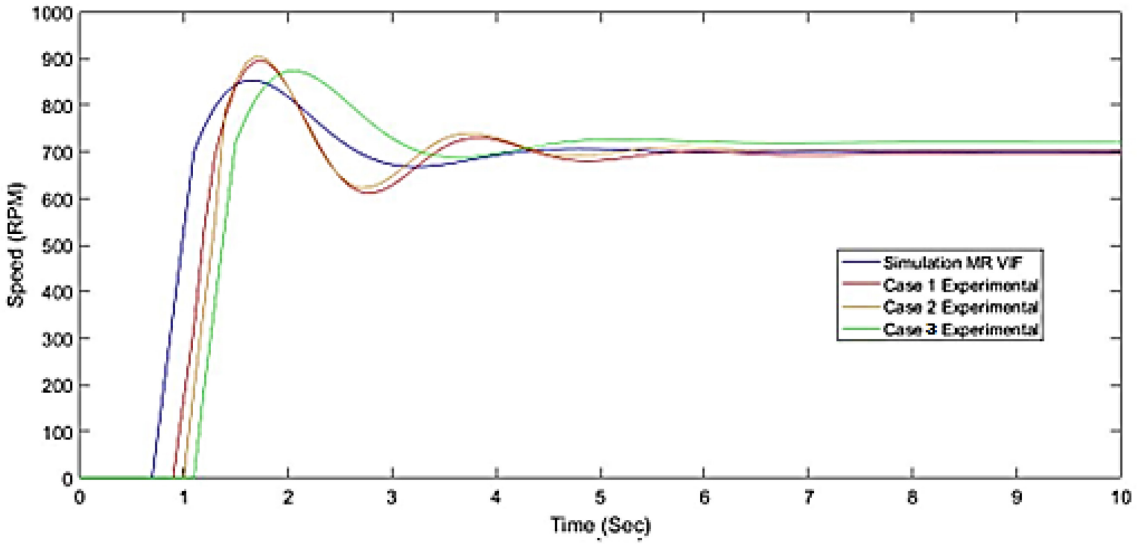

Figure 9. Speed stability analysis for simulation and experimental MRVIF for different case studies

6.2. Power Consumption Analysis of the Model

Two distinct methodologies were employed to determine energy consumption: a short-term approach and a long-term approach, as shown in Figure 10. The short-term difference computation included capturing and documenting readings using camera recording for a duration of 15 to 30 seconds. Subsequently, the recorded values were manually documented. The system operated continuously for an extended duration of around thirty minutes, after which the aggregate power consumption was computed. To examine long-term energy usage, a motor linked with a Fixed Inertia Flywheel (FIF) was operated at various speeds for a duration of thirty minutes. The digital energy meter collected all power consumption data, and the resulting difference is shown in Table 2. The data clearly indicates that there was a significant reduction in power consumption for all scenarios when the magnetorheological (MR) fluid was used to alter the mass position in the variable inertial flywheel (VIF).

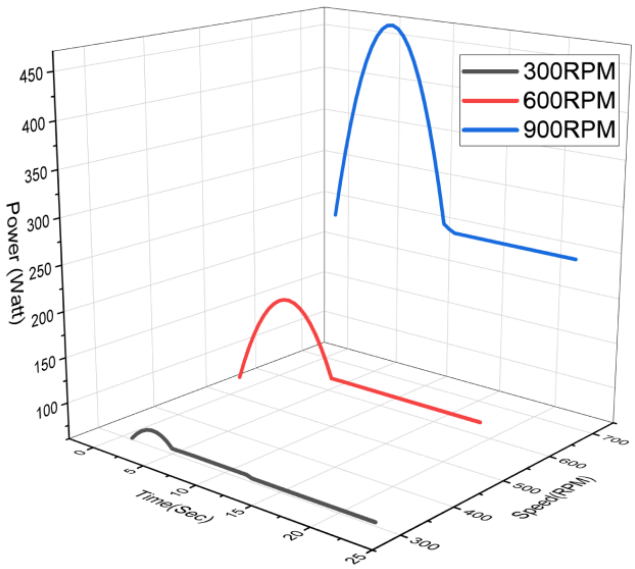

Figure 10. Power consumption representation for different speed of MR VIF

https://doi.org/10.31436/iiumej.v25i2.3094

Table 2. Power consumption analogy with and without MRVIF

Speed RPM	Energy	VIF type			
		VIF	MR Fluid VIF Case 1	MR Fluid VIF Case 2	MR Fluid VIF Case 3
300	Consumed energy in half an hour (kwhr)	44.21	42.37	42.13	42.07
	Maximum power (Watt)	89.9	91.6	92.1	92.3
	Minimum Power (Watt)	86.1	81.2	82.2	81.7
	Average Power (Watt)	88.3	82.85	81.22	81.05
600	Consumed energy in half an hour (kwhr)	112.31	103.64	103.01	101.14
	Maximum power (Watt)	227.6	239.4	239.7	240.1
	Minimum Power (Watt)	217.16	197.1	196.5	196.1
	Average Power (Watt)	220.48	201.47	199.07	198.97
900	Consumed energy in half an hour (kwhr)	237.11	215.55	213.95	211.7
	Maximum power (Watt)	540.13	566.1	569.4	571.2
	Minimum Power (Watt)	436.48	397.21	396.01	395.91
	Average Power (Watt)	464.5	426.2	419.12	416.7

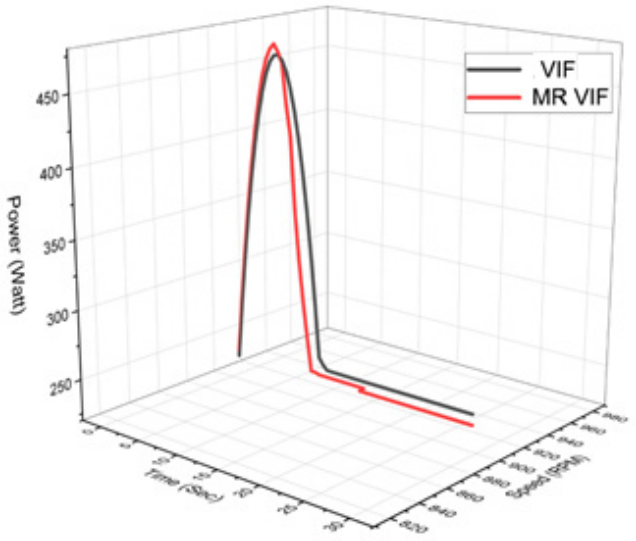

Figure 11. Power consumption representation for 900 RPM speed of MR VIF and VIF

The MR fluid requires activation by an external power source, with an energy consumption of 0.012 kilowatt-hours (kWh) per hour, which may be deemed negligible. Moreover, the power-saving capability exhibited an upward trend as the rotating speed rose.

https://doi.org/10.31436/iiumej.v25i2.3094

6.3. Discussion

The usefulness and stability of the Magneto-Rheological Variable Inertia Flywheel (MRVIF) in regulating rotational speed and limiting power consumption were demonstrated by the results of its experiments. The MR fluid damper in the MRVIF showed accurate corrections to the moment of inertia to changing magnetic fields during a series of dynamic tests. The system's capacity to effectively manage kinetic energy was confirmed by the dynamic control mechanism, which translated into steady and regulated rotating speeds. The trial results also showed a significant decrease in power usage compared to conventional flywheel systems, highlighting the useful advantages of using magnetorheological technology. Overall, the experimental findings confirm the MRVIF's potential as a novel approach to energy-efficient rotational control by offering empirical proof for its effectiveness and stability in practical applications. The close correspondence between the expected and test outcomes is a clear indication of a strong agreement. The factors contributing to minor disparities between them are as follows:

1. During a state of equilibrium, the test results exhibited more variations than their anticipated values. The model did not consider the dynamics of the multi-piston induction motor, the controller's non-linear behaviour, or the forces of MR fluid flow.

2. The model did not consider the MR fluid element's non-linearity. Nevertheless, the disparities between the average values of the steady-state portion of the anticipated and experimental outcomes were minimal.

Their strong relationships validate the assumptions established throughout the model's development. The accuracy of the projected outcomes may have been enhanced by considering the controller detail and the MR fluid. Because of constraints in the test setup design, it was not possible to carry out the experiment using a flywheel with a big diameter. Alternatively, a larger range of operating conditions would have provided improved visibility of the speed fluctuations. The study demonstrates the impact of inertia variation on speed response by simulating models and adjusting the slider position from 0.07 to 0.14m.

Table 3. Comparison of parameters for different case studies

Sl No	Case	Maximum Overshot (%)	Rise Time	Settling Time
1	Simulation	21.9220	0.3200	3.8389
2	Case 1	28.8274	0.3163	4.9763
3	Case 2	28.4227	0.2996	4.8041
4	Case 3	21.3131	0.2719	4.2290

However, the speed response became slower as the viscosity of the MR Fluid increased due to the varying inertia of the flywheel. The system answers were likewise acquired by utilizing the initial power delivered to the controller in all instances. The simulation investigation was also conducted by varying the damping coefficient with different viscosities. Figure 9 displays the temporal responses of the slider position and the variation of the damping coefficient of MR fluid in relation to the slider position for all three situations. The slider rapidly stabilizes as the spring stiffness increases, as depicted in the figure. Nevertheless, the speed of the slider diminished as the viscosity increased, as evidenced by the slope at 1.5 seconds. This is because the slider's change in position was slower when the spring became firmer. The spring force response has a similar pattern to that of the slider position response. As viscosity increases, more power is required to move the sliders. Hence, the speed range of the induction motor expands in proportion to the viscosity of the MR fluid.

The induction motor speeds exhibited lower maximum overshoots (%) when using the MR VIF compared to the VIF shown in Table 2. This signifies that the MR VIF generated reduced levels of vibration, hence enhancing the longevity of the system's components. Thus, it is concluded that by utilizing the MR VIF instead of the VIF, it is possible to decrease the maximum amplitude of vibration and attain a higher steady-state speed. Finally, also for the long running condition, the model consumed less energy if the excitation for the MR VIF was applied. The possible reason for the overall inertia increments for MR fluid addition and the variable inertia mass stayed close to the central position for the higher damping force.

Among the many essential parts of the Magneto-Rheological Variable Inertia Flywheel (MRVIF) is the MR fluid damper. A magnetizable fluid that changes viscosity in reaction to an applied magnetic field powered the MR fluid damper. To dynamically modify the moment of inertia, this damper was carefully included in the flywheel system. The flywheel's rotating speed may be actively controlled by the system by varying the strength of the magnetic field inside the MR fluid damper. The effective management of rotational energy made possible by this dynamic adjustment of inertia promoted the best possible energy storage and release. As a result, the MRVIF is a potential technology for applications as it provides a way to lower power consumption by cleverly adjusting the flywheel's inertial characteristics in real time.

7. CONCLUSION

This article examined and analyzed the dynamic reactions of the induction motor speed driving VIF and MR VIF while maintaining the same maximum inertia values. The system model was constructed utilizing the bond graph simulation methodology, and the resulting equations produced from the model were solved using numerical methods. The experimental validation confirmed the model's transitory behaviour. The MR VIF method demonstrated a significant decrease in peak values of the induction motor speed compared to the VIF method, following a sudden shift in speed. The viscosity of the magnetorheological (MR) fluid in the VIF system directly affected the stability of the speed of the induction motor. These responses are also validated by comparing them with the test data. Minor disparities identified between the projected and actual data necessitate additional improvement of the model and the utilization of sensors with a higher sampling rate and more advanced data-gathering technology. Additionally, the system displayed a significant decrease in power consumption. While the construction of MR VIF was more intricate than VIF, it effectively decreased the maximum amplitude of vibration and thus reduced the system's speed.

Also, energy storage and rotational control systems might be completely transformed by implementing energy-saving and speed stability in Magneto-Rheological Variable Inertia Flywheels (MRVIF) in industrial settings. Using MR fluid dampers to dynamically modify the moment of inertia, the MRVIF provides accurate control over rotational speed, guaranteeing stability in industrial operations. This flexibility improves operational dependability while simultaneously optimizing energy usage. This technique might be applied in the real world to a variety of industrial systems, including production lines, grid stability, and installations for renewable energy. Significant power consumption savings, increased efficiency, and increased stability in the face of fluctuating loads or disturbances are among the implications.

REFERENCES

[1] V. Kartašovas, V. Barzdaitis, and P. Mažeika, “Modeling and simulation of variable inertia rotor,” *J. Vibroengineering*, vol. 14, no. 4, pp. 1745–1750, 2012.

[2] X. Dong, J. Xi, P. Chen, and W. Li, “Magneto-rheological variable inertia flywheel,” *Smart Mater. Struct.*, vol. 27, no. 11, p. 115015, Nov. 2018, doi: 10.1088/1361-665X/aad42b.

[3] C. Jauch, "Controls of a flywheel in a wind turbine rotor," *Wind Eng.*, vol. 40, no. 2, pp. 173–185, 2016, doi: 10.1177/0309524X16641577.

[4] M. Huang, "Optimization of powered wheels for commercial aircraft and design of test scheme," *Proc. Inst. Mech. Eng. Part D J. Automob. Eng.*, vol. 237, no. 7, pp. 1751–1764, Jun. 2023, doi: 10.1177/09544070221093182.

[5] M. Malekan, A. Khosravi, and X. Zhao, "The influence of magnetic field on heat transfer of magnetic nanofluid in a double pipe heat exchanger proposed in a small-scale CAES system," *Appl. Therm. Eng.*, vol. 146, pp. 146–159, 2019, doi: 10.1016/j.applthermaleng.2018.09.117.

[6] L. Islam, M. M. Rashid, and M. A. Faysal, "Investigation of the Energy Saving Capability of a Variable Inertia Magneto-Rheological (MR) Flywheel," vol. 2, no. 1, pp. 25–31, 2022.

[7] S. M. Salam and M. M. Rashid, "A new approach to analysis and simulation of flywheel energy storage system," in *8th International Conference on Mechatronics Engineering (ICOM 2022)*, 2022, pp. 90–94, doi: 10.1049/icp.2022.2271.

[8] W. Lu, Y. Luo, L. L. Kang, and D. Wei, "Characteristics of magnetorheological fluids under new formulation," *J. Test. Eval.*, vol. 47, no. 4, 2019, doi: 10.1520/JTE20170477.

[9] T. Liu, J.; Miura, Y.; Ise, "Comparison of dynamic characteristics between virtual synchronous generator and droop control in inverter-based distributed generators," *IEEE Trans. Power Electron.*, vol. 31, pp. 3600–3611, 2015.

[10] C. Li, M. Liang, and T. Wang, "Criterion fusion for spectral segmentation and its application to optimal demodulation of bearing vibration signals," *Mech. Syst. Signal Process.*, vol. 64–65, pp. 132–148, Dec. 2015, doi: 10.1016/j.ymssp.2015.04.004.

[11] D. Richiedei, A. Trevisani, and G. Zanardo, "A Constrained Convex Approach to Modal Design Optimization of Vibrating Systems," *J. Mech. Des.*, vol. 133, no. 6, Jun. 2011, doi: 10.1115/1.4004221.

[12] D. J. Inman, *Engineering Vibration*, Internatio. Prentice-Hall International, Inc, 1994.

[13] T. E. Saaed, G. Nikolakopoulos, J. E. Jonasson, and H. Hedlund, "A state-of-the-art review of structural control systems," *JVC/Journal Vib. Control*, vol. 21, no. 5, pp. 919–937, 2015, doi: 10.1177/1077546313478294.

[14] M. Trikande, N. Karve, R. Anand Raj, V. Jagirdar, and R. Vasudevan, "Semi-active vibration control of an 8x8 armored wheeled platform," *J. Vib. Control*, vol. 24, no. 2, pp. 283–302, Jan. 2018, doi: 10.1177/1077546316638199.

[15] G. W. Housner *et al.*, "Structural Control: Past, Present, and Future," *J. Eng. Mech.*, vol. 123, no. 9, pp. 897–971, 1997, doi: 10.1061/(asce)0733-9399(1997)123:9(897).

[16] S.-G. Luca, F. Chira, and V.-O. Rosca, "Passive Active and Semi-Active Control Systems in Civil Engineeering," *Constr. Arhit.*, vol. 3, p. 4, 2005.

[17] N. Eslaminasab, "Development of a Semi-active Intelligent Suspension System for Heavy Vehicles," p. 181, 2008.

[18] Thoma JU., "Simulation by bondgraphs: Introduction to a graphical method," *Berlin Springer Sci. Bus. Media*, 2012.

[19] M. T. Fan Y, Mu A, "Study on the application of energy storage system in offshore wind turbine with hydraulic transmission," *Energ Convers Manag. 2016*, pp. 338–346, 2016.

[20] E. P. Kat C-J, "Validation metric based on relative error," *Math Comp Model Dyn*, vol. 18(5), pp. 487–520, 2012.